Particle-Filter-Based Radio Localization for Mobile Robots in the Environments With Low-Density WLAN APs

Bing-Fei Wu, *Fellow, IEEE*, and Cheng-Lung Jen

***Abstract*—This paper proposes a new localization method for mobile robots based on received signal strength (RSS) in indoor wireless local area networks (WLANs). In indoor wireless networks, propagation conditions are very difficult to predict due to interference, reflection, and fading effects. As a result, an explicit measurement equation is not available. In this paper, an observation likelihood model is accomplished using kernel density estimation to characterize the dependence of location and RSS. Based on the measured RSS, the robot's location is dynamically estimated using the proposed adaptive local search particle filter (ALSPF), which adopts the covariance adaptation for correcting the system states and updating the motion uncertainty. To deal with low sensor density in large-space environments, we present a strategy based on the strongest signal with minimum variance to choose a subset of detectable access points (APs) for enhancing robot localization and reducing the computational burden. The proposed approaches are verified by realistic low-density WLAN APs to demonstrate the feasibility and suitability. Experimental results indicate that the proposed ALSPF provides approximately 1-m error and significant improvements over particle filtering.**

***Index Terms*—Kernel density estimation (KDE), particle filter (PF), robot localization, wireless local area network (WLAN).**

I. Introduction

In recent years, mobile robots have been increasingly being used in a wide range of indoor services [1], [2] and human interaction [3], [4] applications such as domestic services [5], security [6], and rehabilitation [7]. To achieve this autonomy, localization is one of the greatest challenges that need to be overcome in order for mobile robots to achieve successful autonomous navigation and perform their intended tasks without human intervention. Accordingly, mobile robots should be able to determine their position and orientation by perceiving their environment using the sensors with which they are equipped or by means of fusion with the infrastructure. Many popular robot localization systems apply the sensors such as vision [8] and range finders [9]. Their performance might be degenerated by obstacles.

Recently, several kinds of radio-based localization solutions have been developed using existing wireless infrastructures such as radio frequency identification (RFID) [10], wireless sensor networks (WSNs) [11], and wireless local area networks (WLANs) [12]. The different wireless location systems utilize different types of radio frequency measurements, such as time of flight (TOF), time difference of arrival, and received signal strength (RSS) [10], [12]. Solutions using delays or angle measurements are complex and not widespread because the specific hardware is too expensive or fragile in cluttered and dynamic environments. Conversely, RSS-based approaches have received more acclaim as RSS values are easily obtained in wireless networks. In addition, WLANs have become a critical enhancement to public spaces, and wireless information access based on IEEE 802.11 is now widely available, and the RSS sensor function is available in every 802.11 interface [12]. As a result, WLAN-based indoor localization is being considered a feasible solution. Many successful solutions are presented in [25], [28]–[30], and [35]–[37].

In this paper, we consider the localization of the mobile robots in practical WLAN environments in which only a few access points (APs) are available. The chief difficulty in this critical condition is predicting RSS and dealing with its non-Gaussian noise from interference, reflection, and fading effects in non-line-of-sight (NLOS) environments. We present a WLAN-RSS fingerprint-based robot localization system. In the offline phase, kernel density estimation (KDE) [41] based on the RSS training set is proposed to build the observation likelihood model for radio map since an explicit measurement model is unknown due to the complexity of indoor environments. In the online phase, to solve the problem of only few APs being detectable in low sensor density and large space, we propose an approach that uses the strongest signal and minimum variance (SSMV)-based AP selection procedure to choose a subset of detectable APs such that the information of all APs is more efficiently utilized.

Moreover, a particle filter (PF) framework that is based on sequential Monte Carlo (SMC) [14] is used to dynamically track the robot's position. In addition, to deal with some cases in which most of the particles are prematurely concentrated and losing diversity, we propose the adaptive local search PF (ALSPF), which utilizes an *adaptive local search* (ALS) algorithm to improve importance sampling and updates the motion uncertainties using the adapted empirical covariance. The following contributions are made in this work.

- A simple online radio map model using KDE, which includes the uncertainties from the environment, is

Manuscript received April 15, 2012; revised November 6, 2012, May 11, 2013, August 8, 2013, and November 18, 2013; accepted March 5, 2014. Date of publication May 30, 2014; date of current version September 12, 2014. This work was supported by the National Science Council of Taiwan under Grant NSC 102-2221-E-009-141.

The authors are with the Institute of Electrical Control Engineering, National Chiao Tung University, Hsinchu 300, Taiwan (e-mail: bwu@cc.nctu.edu.tw).

Color versions of one or more of the figures in this paper are available online at http://ieeexplore.ieee.org.

Digital Object Identifier 10.1109/TIE.2014.2327553

developed based only on RSS training pairs, instead of building models that require extensive training effort for parameter learning or fine-grained interpolation.
- An AP selection algorithm that selects the strongest APs with smallest variance is proposed to deal with the noisy NLOS propagation by the pedestrians or obstacles. Our approach simultaneously reduces online computation complexity, enhances global localization, and presents the robustness to fewer APs applicable conditions.
- To enhance the accuracy, the proposed ALSPF is not only based on the PF framework but also provides an ALS to eliminate unreasonable estimates, instead of using an exhaustive global resampling search, while presenting approximately 1-m accuracy using only two APs with high motion velocity.

Moreover, the amount and the scenario of the examined routes are practical enough to be compared with related work on radio-based robot localization [10], [15], [16], [18], [21], [24].

The remainder of this paper is organized as follows. In Section II, we address related work and the problems to be resolved. Section III gives a problem formulation of WLAN-based robot localization. Section IV describes the proposed radio localization systems. Section V presents the radio map modeling using KDE. Section VI presents our experiments and results. Finally, we conclude this paper in Section VII.

II. Related Work

In WLAN positioning, the techniques can be categorized into *range-based positioning* [13], [15], [20], [23] and *location fingerprinting* [12], [25], [26], [28]–[30], [33], [35] [37]. The range-based approaches rely on range measurements that compute the position of a mobile terminal based on the wireless measurements with some base stations whose locations are given. Distances can be converted from either RSS or time-based methods with TOF measurements. The multilateration approach [12] based on some propagation models only can be applied for static or very slow motion conditions of mobile terminals. Recently, many applications using this scheme for chirp spread spectrum (CSS)-based localization systems have been proposed [19]–[21] since the distances between mobile CSS tags can be simply measured with the CSS base stations fixed at known coordinates. However, in reality, this requires complex network infrastructure, which is not presented in today's conventional network installations. Recently, ultrasonic signals also have been mainly used for indoor localization due to their low cost and simple installation [17], [22]–[24]. The addressed propagation models are sensitive to disturbances, i.e., the faster the mobile terminal moves, the more the localization errors increase.

In addition, range-based methods are forced to deal with bias and the noisy distance due to the interference in NLOS environments. Most of existing solutions for radio-based robot localization assume requiring high sensor density and slow velocity and are usually tested in simple environments, which might not be suitable for practical application.

In WLANs, the most feasible solution for RSS-based localization is the location fingerprinting [25]. This method directly uses a radio map to characterize the RSS–position relationship through training measurements at anchor points (ANs) without the assumption of isotropic RSS contours, invariance to receiver orientation, and exact knowledge of AP locations. Fingerprinting consists of offline and online stages; during the offline stage, RSS is collected at ANs to build the radio map. In the online stage, the mobile terminal location is estimated by matching RSS in the radio map [25], [28], [29]. Since RSS can be used in most wireless devices, mobile robots are able to measure the RSS with WLAN adapters to facilitate the robot localization [30], [37], [38].

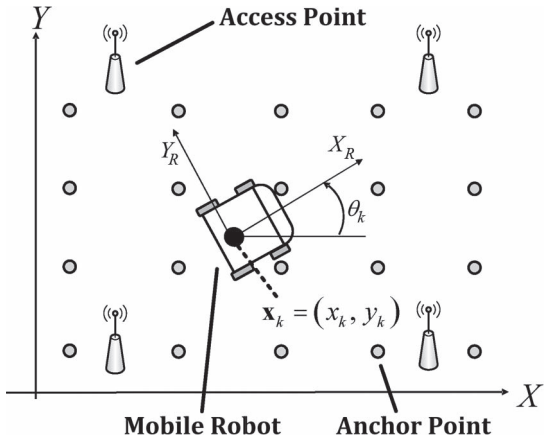

Fig. 1. WLAN environment and task space for a mobile robot. A number of APs are installed in the area, and the mobile robot is equipped with a mobile device (such as a smartphone or a laptop) to receive WLAN-RSS values for localization.

III. Problem Statement

In this paper, our primary focus is on the radio localization of mobile robots through RSS readings with low-density WLAN. As depicted in Fig. 1, we want to track the position of the mobile robot using WLAN-RSS measurements. In our work, there is no need for the locations that are equipped with APs to be known—which is more practical for real applications. Based on the location fingerprinting, the WLAN-RSS values are collected as training pairs at each AN to build radio map models using KDE. A number of commercial off-the-shelf APs are installed in the testbed, and the mobile robot is equipped with a mobile device to receive the WLAN-RSS measurements.

Fig. 2 gives an overview of the proposed radio-based robot localization system, which is divided into two phases: an offline training phase and an online estimation phase. In the training phase, determination of the dependence between the RSS and a certain location is carried out. This is a challenging task in indoors due to radio interference, multipath fading, shadowing, and NLOS caused by indoor propagation. Because the WLAN-RSS values are measured in a complex environment, we propose the use of a nonparametric regression scheme based on KDE to extend the flexibility of location fingerprints as the sensed RSS in the online stage may not be accurate but is relevant to the neighborhood.

As shown in Fig. 2, the work is in two phases and is based on the location fingerprints that use a radio map to implicitly characterize the RSS–position relationship through training

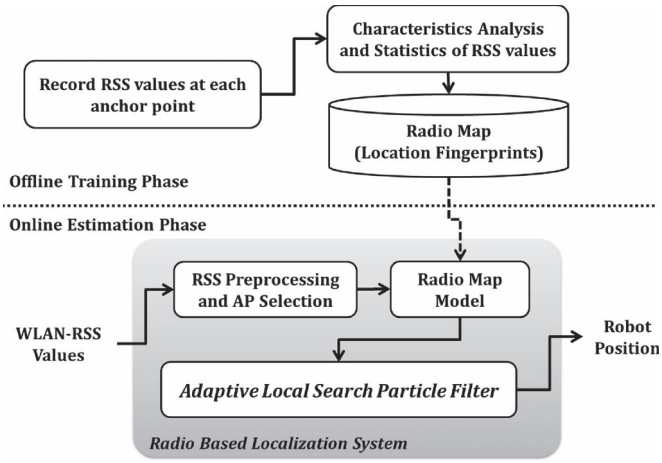

Fig. 2. Schematic of the proposed localization scheme. In the offline phase, a training stage is proceeded to build the radio map, and an ALSPF is provided to dynamically estimate the robot position in real time.

measurements at ANs with known coordinates [30]. In the offline training phase, the radio localization works as follows: Given a set of base station APs in WLAN $\mathcal{B} = \{b_1, b_2, \ldots, b_{N_B}\}$, each capable of transmitting radio signals periodically in a field $\mathcal{F} \subseteq \Re^2$, where N_B is the total number of base stations (i.e., APs) installed in the task space, in the offline training phase, we measure the signal strengths at each AN to build a *radio map* that is a set $\mathcal{R} = \{\mathbf{x}_{\rm tr}^i, \mathbf{r}_\mu^i, \mathbf{r}_\sigma^i\}_{i=1}^{N_{\rm AN}}$, where $N_{\rm AN}$ is the total number of ANs, $l_i \in \Re^2$ is the known training location (also called the AN) labeled by 2-D Cartesian coordinates $\mathbf{x}_{\rm tr}^i = [x_{{\rm tr},x}^i \; x_{{\rm tr},y}^i]^T$, $\mathbf{r}_\mu^i = [r_{\mu,1}^i, \ldots, r_\mu, N_B^i]^T$, $r_{\mu,j}^i$ is the averaged RSS vector at $\mathbf{x}_{\rm tr}^i$ from b_j in $\mathcal{B}$, $\mathbf{r}_\sigma^i = [r_{\sigma,1}^i, \ldots, r_{\sigma,N_B}^i]^T$, and $r_{\sigma,j}^i$ is the RSS standard deviation vector at $\mathbf{x}_{\rm tr}^i$ from b_j, $j = 1, \ldots, N_B$.

During the online estimation phase, a new RSS observation $\mathbf{r}_k$ is measured by the mobile device equipped on the robot, where $k \in \Re$ is the time instant, $\mathbf{r}_k = [r_{k,1}, \ldots, r_{k,N_{\rm DB}}]^T$ contains RSS measurements from $N_{{\rm DB},k}$ APs at time k, and $r_{k,j}$ is the received RSS value from b_j $(j = 1, \ldots, N_{{\rm DB},k}$, and $N_{{\rm DB},k}$ is the number of detectable AP at time $k)$. The set $\mathcal{R} = \{\mathbf{x}_{\rm tr}^i, \mathbf{r}_\mu^i, \mathbf{r}_\sigma^i\}_{i=1}^{N_{\rm AN}}$ is collected in a database in the offline phase to construct the probabilistic observation likelihood by KDE for the online phase to determine the sample importance weights.

IV. Proposed Radio Localization Algorithms

Here, we present details on the proposed radio localization system. To enhance the robustness of estimation, the ALS algorithm is involved in the resampling to dynamically correct motion uncertainties by updating the empirical covariance matrix. In addition, an AP selection strategy is proposed to improve estimation stability.

A. Standard PF

In this paper, we assume that the robot lies on a planar indoor environment and that its position is described by a vector $\mathbf{x}_k \in \Re^{n_x}$, which is defined as

$$\mathbf{x}_k = [x_k \quad y_k]^T$$

where n_x is the dimension of state. At each time instant k, sensors deliver measurements $\mathbf{z}_k \in \Re^{n_z}$ for the robot. The aim is to provide an estimate $\hat{\mathbf{x}}_k$ of the state $\mathbf{x}_k$. Based on the assumption of Markovian dynamics, the system dynamical model and measurement model are defined by

$$\mathbf{x}_k = f(\mathbf{x}_{k-1}, \mathbf{w}_k) \tag{1}$$

$$\mathbf{z}_k = h(\mathbf{x}_k, \mathbf{v}_k) \tag{2}$$

where $f(\cdot) : \Re^{n_x} \times \Re^{n_w} \to \Re^{n_x}$ is referred to as the transition function of state $\mathbf{x}_{k-1}$, and $h(\cdot) : \Re^{n_x} \times \Re^{n_v} \to \Re^{n_z}$ is referred to as the measurement function. Furthermore, $\mathbf{w}_k$ and $\mathbf{v}_k$ are the discrete white zero-mean noise processes, i.e., $\mathbf{w}_k \sim N(0, Q)$ with covariance matrix $Q = {\rm diag}(\sigma_x^2, \sigma_y^2)$ and $\mathbf{v}_k \sim N(0, R)$ with covariance matrix $R = {\rm diag}(\sigma_{r,1}^2, \ldots, \sigma_{r,N_{\rm DB}}^2)$.

The SMC approach is an approximation technique for solving the Bayesian filtering problem by representing $p(\mathbf{x}_k|\mathbf{z}_{1:k})$ using a set of N_S samples of the state space (particles) with associated weights. At the time instant k, a set of particles is defined by

$$S_k = \left\{ \left(\mathbf{x}_k^i, \omega_k^i\right) | i = 1, \ldots, N_S \right\}$$

where $\mathbf{x}_k^i = [x_k^i \; y_k^i]^T \in \Re^2$ and $\omega_k^i \in \Re$ denote the ith particle state and the associated importance weight, respectively. The weights are normalized such that $\sum_i \omega_k^i = 1$.

Based on the linear velocity v_k provided by encoders and heading angle θ_k measured by using an inertial measurement unit (IMU) with compass, a particle containing the robot position in 2-D space at time instant k and the particle motion can be predicted by the following equation:

$$\mathbf{x}_k^i = f\left(\mathbf{x}_{k-1}^i\right) + \mathbf{w}_k = \mathbf{x}_{k-1}^i + \begin{bmatrix} v_k \cdot T_S \cdot \cos\theta_k \\ v_k \cdot T_S \cdot \sin\theta_k \end{bmatrix} + \mathbf{w}_k \tag{3}$$

where T_S represents the sampling time of 2-D motion of the robot, and the noise covariance matrix $Q = {\rm diag}(T_s^2/2, T_s^2/2)$. The expectation of state estimate $\hat{\mathbf{x}}_{k|k-1}$ also can be obtained by

$$\hat{\mathbf{x}}_{k|k-1} = f(\hat{\mathbf{x}}_{k-1|k-1}) \tag{4}$$

$$P_{k|k-1} = \sum_{i=1}^{N_S} \omega_k^i \cdot \left[\mathbf{x}_k^i - \hat{\mathbf{x}}_{k|k-1}\right] \left[\mathbf{x}_k^i - \hat{\mathbf{x}}_{k|k-1}\right]^T + Q. \tag{5}$$

The posterior $p(\mathbf{x}_k|\mathbf{z}_{1:k})$ and the system state $\hat{\mathbf{x}}_{k|k}$ can now be approximated [14] by the following equations:

$$p(\mathbf{x}_k|\mathbf{z}_{1:k}) \approx \sum_{i=1}^{N_S} \omega_k^i \cdot \delta\left(\mathbf{x}_k - \mathbf{x}_k^i\right) \tag{6}$$

$$\hat{\mathbf{x}}_{k|k} = \mathbb{E}[\mathbf{x}_k|\mathbf{z}_{1:k}] = \int \mathbf{x}_k \cdot p(\mathbf{x}_k|\mathbf{z}_{1:k}) d\mathbf{x}_k \approx \sum_{i=1}^{N_S} \omega_k^i \cdot \mathbf{x}_k^i \tag{7}$$

$$P_{k|k} = \sum_{i=1}^{N_S} \omega_k^i \cdot \left[\mathbf{x}_k^i - \hat{\mathbf{x}}_{k|k}\right] \left[\mathbf{x}_k^i - \hat{\mathbf{x}}_{k|k}\right]^T \tag{8}$$

where $\delta(\cdot)$ is the Dirac delta function.

B. Proposed ALSPF

In the SMC algorithm, the choice of the proposal distribution $q(\mathbf{x}_k^i|\mathbf{x}_{k-1}^i, \mathbf{z}_k)$ directly impacts the efficiency. Reference [14] provides a straightforward choice of proposal distribution for importance sampling as follows:

$$q\left(\mathbf{x}_k^i|\mathbf{x}_{k-1}^i, \mathbf{z}_k\right) = p\left(\mathbf{x}_k^i|\mathbf{x}_{k-1}^i, \mathbf{z}_k\right) = p\left(\mathbf{x}_k^i|\mathbf{x}_{k-1}^i\right) \tag{9}$$

with weight

$$\omega_k^i = \omega_{k-1}^i \cdot p\left(\mathbf{z}_k|\mathbf{x}_k^i\right). \tag{10}$$

The dynamism of indoor propagation, however, causes radio conditions to deviate from the RSS map [30], [33]. With the PF, most of the particles occasionally prematurely concentrate at a wrong point induced by noise-disrupted RSS observations and thereby losing diversity and resulting in failed estimations. Two conditions that occur in online estimation processes are taken account as follows.

1) *Particle degeneracy (PD)*: A common problem with the PF is degeneracy, which implies that a large amount of computational effort is devoted to updating particles whose contribution to the approximation to $p(\mathbf{x}_k|\mathbf{z}_{1:k})$ is zero. A suitable measure of degeneracy of the algorithm is the effective sample size $\hat{N}_{\text{eff}}$ [14], i.e.,

$$\hat{N}_{\text{eff}} = \frac{1}{\sum_{n=1}^{N_S} \left(\omega_k^n\right)^2}. \tag{11}$$

2) *Infeasible estimate (IE)*: In dynamical environments, the WLAN-RSS, robot velocity, and orientation might be disturbed by unpredictable noise, which causes the state to be predicted to an infeasible region, as shown in Fig. 3(a).

To improve the robustness of importance sampling, the proposed ALS algorithm is a one-step search procedure, which can be used for detecting feasibility (PD and IE). Hence, the ALS algorithm mitigates the adverse effects of environmental noise and corrects the estimated states. The proposed ALSPF utilizes an adaptively local varying area to search for a more reasonable estimate based on the recent motion velocity. This releases the limitation of the search area based on fixed uncertainty statistics by PF at the failed estimation instants. The illustration for ALSPF is presented as follows.

1) *Detect IE*: Fig. 3(a) shows that the robot location is predicted to be in an infeasible region; thus, particles will be degenerated at this region.
2) *Evaluate ALS region* $\mathcal{A}$: Instead of proceeding using global resampling, which is an exhaustive search that will cause a high estimation variance, we propose an ALS strategy to efficiently evaluate a new result of estimation at time instant k. The search strategy is done in accordance with an ALS region that is determined by the average of the robot velocity to compute the boundary of the area $\mathcal{A} \subseteq \Re^2$ and is defined as follows:

$$\mathcal{A} = \{(x, y)|A_{XL} \le x \le A_{XU},\ A_{YL} \le y \le A_{YU}\} \tag{12}$$

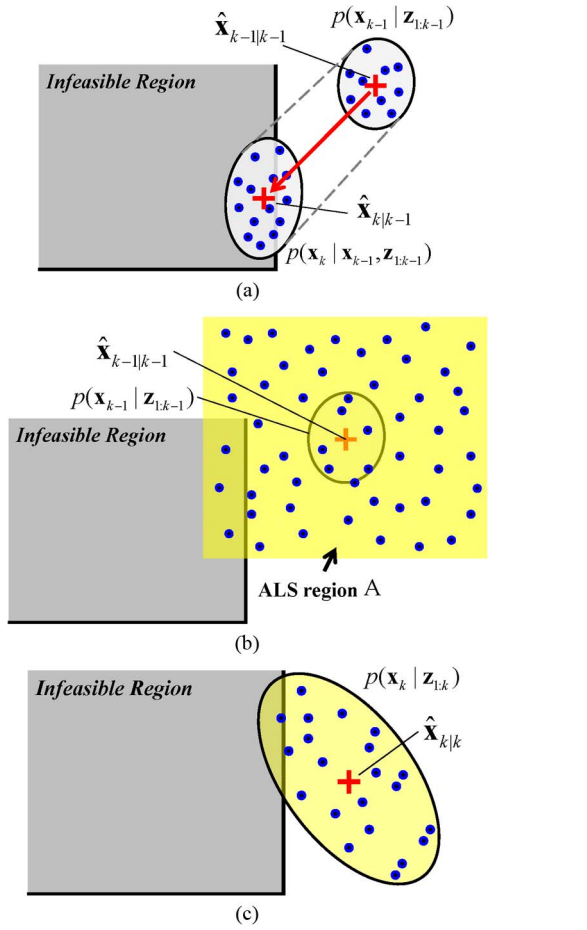

Fig. 3. Illustration of the proposed ALS algorithm. (a) IE condition occurs due to noisy measurements. (b) IE condition is detected, and the ALS algorithm is performed by expanding a reasonable area to search for a better solution (a one-step search). (c) Evaluation of a new estimate and covariance by the surviving particles.

where

$$\begin{cases} A_{XL} = \hat{x}_{k-1|k-1} - \bar{v}_k \cdot T_{\text{ALS}} \\ A_{XU} = \hat{x}_{k-1|k-1} + \bar{v}_k \cdot T_{\text{ALS}} \end{cases} \tag{13}$$

$$\begin{cases} A_{YL} = \hat{y}_{k-1|k-1} - \bar{v}_k \cdot T_{\text{ALS}} \\ A_{YU} = \hat{y}_{k-1|k-1} + \bar{v}_k \cdot T_{\text{ALS}} \end{cases} \tag{14}$$

and T_{ALS} is a time window that depends on the sensor sampling rate, and $\bar{v}_k$ is an averaged linear velocity. Based on the computed searching area $\mathcal{A}$, the particles are generated in the area using a uniform sampling such that $\mathbf{x}_k^i = [x_k^i\ y_k^i]^T,\ i = 1, \ldots, N_S \in \mathcal{A}$ with

$$x_k^i \sim U(A_{XL}, A_{XU})\ \ y_k^i \sim U(A_{YL}, A_{YU}), \quad i = 1, \ldots, N_s. \tag{15}$$

3) *Update the estimate*: In Fig. 3(c), after sampling at the ALS area $\mathcal{A}$, the particles are selected by evaluating the observation likelihood $p(\mathbf{z}_k|\mathbf{x}_k^i)$. As a result, the new particle set $S_k' = \{(\mathbf{x}_k^i, \omega_k^i)|i = 1, \ldots, N_S'\}$ can be

TABLE I
ALGORITHM 2: ADAPTIVE LOCAL SEARCH PARTICLE FILTER

- Draw N samples from the importance distribution:
  - **Prediction**: $\mathbf{x}_k^i \sim p(\mathbf{x}_k \mid \mathbf{x}_{k-1}^i, \mathbf{z}_{1:k-1})$, $i = 1,...,N_S$
- IF location estimate $\hat{\mathbf{x}}_{k|k-1}$ is infeasible or $\hat{N}_{eff} < N_T$:
  - **Perform ALS**: Calculate ALS region $\mathcal{A}$ using (13) and (14).
  - Draw N_S samples in the adaptive search region by uniform random number generation using (15).
  - **Importance sampling in ALS region** $\mathcal{A}$: Assign the particle a weight, $\omega_k^i = p(\mathbf{z}_k \mid \mathbf{x}_k^i)$.
  - **Resampling**: Roulette-wheel resampling.
  - **ALS Update**: Calculate sample mean and empirical covariance from the selected N_S' samples to compute $\hat{\mathbf{x}}_{k|k}$ and the empirical covariance $P_{k|k}$ using (16) and (17).
  - **Uncertainty Update**: Use $\eta^2 P_{k|k}$ to update the process uncertainties (1).
- ELSE
  - **Importance sampling**: Assign the particle a weight: $\omega_k^i = p(\mathbf{z}_k \mid \mathbf{x}_k^i)$, $i = 1,...,N_S$.
  - **Update**: Calculate $\hat{\mathbf{x}}_{k|k}$ and $P_{k|k}$ using (16) and (17).
  - **Resampling**: Roulette-wheel resampling.
- END IF

provided, and the new sample mean and empirical covariance are computed as follows:

$$\hat{\mathbf{x}}_{k|k} \approx \sum_{i=1}^{N_S'} \omega_k^i \cdot \mathbf{x}_k^i \tag{16}$$

$$P_{k|k} = \sum_{i=1}^{N_S'} \omega_k^i \cdot \left[\mathbf{x}_k^i - \hat{\mathbf{x}}_{k-1|k-1}\right]\left[\mathbf{x}_k^i - \hat{\mathbf{x}}_{k-1|k-1}\right]^T. \tag{17}$$

4) *Evaluate the process uncertainty*: We utilize the results in Fig. 3(c) and the covariance matrix $P_{k|k}$ in (17) to update the robot motion process uncertainties by using $\eta^2 P_{k|k}$ to update σ_x^2 and σ_y^2, where η is a confidence level or a scalable step size for the state prediction.

Consequently, the ALSPF algorithm is used to enhance the importance sampling by anticipating the PD problem and adapting its covariance accordingly to mitigate deviated estimates. The complete ALSPF algorithm is summarized in Table I.

C. Base Station Selection Strategies

Until recently, many researchers have studied how to improve the positioning efficiency while achieving an acceptable accuracy. This motivates the need for AP selection techniques in WLAN positioning [25]–[33], [37], [39]. Reference [31] first utilized the subset of APs to reduce the computational cost for APs with the strongest signal. Discriminant-based approaches can provide a subset of APs to reduce complexity and ensure the most discriminative view of the RSS environment [27], [30], [32]. Reference [30] offers an AN-based AP selection technique that uses the Fisher criterion as the selection criterion and minimizes the correlation between the selected APs. Nevertheless, for a low-sensor-density case, it might be inappropriate to choose APs according to the offline AN since the online RSS observations vary dramatically.

In this context, we explore robot localization in low-AP-density WLAN environments. In such a density-constrained condition, the accuracy of localization is highly dependent on the precision of sensor measurements. The APs with weak signal strengths or unstable linkages should be excluded in the online positioning stage. Therefore, we propose a strategy based on the strongest RSS mean with minimum variance to choose a subset of detectable APs to be the source of observations of the radio localization. The goal of Steps 1–3 in Table II is primarily to find the AP that has stronger strength mean. In (18), it provides a moving averaged RSS observation vector (Step 1). Accordingly the strength can be ordered (Step 2), and weak APs should be ignored. Then, a subset of stronger APs is chosen (Step 3). Therefore, Steps 4–6 in Table II proceed to select a set of stable APs from the results of Step 3 with a stable observation measure using (19). Finally, Step 6 outputs the set of base stations that are used for the online estimation. In general positioning techniques, the estimation approach requires at least three base stations, whereas the proposed SSMV-based radio localization system only requires two.

TABLE II
ALGORITHM 3: STRONGEST SIGNAL WITH MINIMUM VARIANCE FOR BASE STATION SELECTION

- **Inputs**: At time instant k, the RSS observation set $\{\mathbf{r}_{k-N_W}, ...\mathbf{r}_k\}$, where N_W is a window frame size, and $\mathbf{r}_k = [r_{k,1} \ldots, r_{k,N_B}]^T$, where N_B is the total number of APs.
- **Step 1)** Compute the moving averaged RSS $\overline{\mathbf{r}}_k = [\overline{r}_{k,1} \ldots, \overline{r}_{k,N_B}]^T$ using

$$\overline{\mathbf{r}}_k = \frac{1}{N_W} \sum_{n=0}^{N_W-1} \mathbf{r}_{k-n} \tag{18}$$

- **Step 2)** Rank APs form the set $\{\overline{r}_{k,1}, \ldots, \overline{r}_{k,N_B}\}$ into $\{\overline{r}_{k,1}^{\max}, \ldots, \overline{r}_{k,N_B}^{\max}\}$ in descending order of mean value $\overline{r}_{k,i}$, $i = 1, \ldots, N_B$, then determine a ranking index from $\{\overline{r}_{k,1}^{\max}, \ldots, \overline{r}_{k,N_B}^{\max}\}$ for base stations:
  - $\mathcal{B}_{index}^{\max} : \{B_1^{\max}, ..., B_{N_B}^{\max}\}$
- **Step 3)** Select M measurement vectors from $\{\mathbf{r}_{k-N_W}, ...\mathbf{r}_k\}$ to be the set that $\{\mathbf{r}_{k-N_W:k,B_1^{\max}} \ldots, \mathbf{r}_{k-N_W:k,B_M^{\max}}\}$ by referring the order of $\mathcal{B}_{index}^{\max}$ into a $M \times N_W$ dimension RSS matrix $\mathbf{Z}_k^{\max}$:
  - $\mathbf{Z}_k^{\max} = [\tilde{\mathbf{z}}_1^{\max}, \ldots, \tilde{\mathbf{z}}_M^{\max}]^T = [\mathbf{r}_{k-N_W:k,B_1^{\max}}, \ldots, \mathbf{r}_{k-N_W:k,B_M^{\max}}]^T$,
    where $\tilde{\mathbf{z}}_1^{\max} = [\tilde{z}_{1,1}^{\max}, ..., \tilde{z}_{1,N_W}^{\max}]^T$, $N_B > M > M_{\min}$, $M, M_{\min} \in \Re$.
- **Step 4)** Compute the RSS variance for $\{\tilde{\mathbf{z}}_1^{\max}, \ldots, \tilde{\mathbf{z}}_M^{\max}\}$ using the following:

$$\begin{bmatrix} \tilde{s}_1 \\ \vdots \\ \tilde{s}_M \end{bmatrix} = \begin{bmatrix} Cov(\tilde{\mathbf{z}}_1^{\max}) \\ \vdots \\ Cov(\tilde{\mathbf{z}}_1^{\max}) \end{bmatrix} = \frac{1}{N_w - 1} \begin{bmatrix} \sum_{n=1}^{N_w} [\tilde{z}_{1,n}^{\max} - \overline{\mathbf{z}}_1^{\max}]^2 \\ \vdots \\ \sum_{n=1}^{N_w} [\tilde{z}_{M,n}^{\max} - \overline{\mathbf{z}}_M^{\max}]^2 \end{bmatrix} \tag{19}$$

- **Step 5)** Rank the set $\{\tilde{s}_1, \ldots, \tilde{s}_M\}$ in ascending order and determine a ranking index set with an ascending order of variance $\{\tilde{s}_1, \ldots, \tilde{s}_M\}$:
  - $\mathcal{B}_{index}^{\min} : \{B_1^{\min}, ..., B_M^{\min}\}$
- **Step 6)** Select m measurements by referring the order of $\mathcal{B}_{index}^{\min}$
  - Produce $\mathbf{z}_k = [r_{k,B_1^{\min}} \ldots, r_{k,B_m^{\min}}]^T$, $m < M, m \in \Re$.

V. RADIO MAP MODELING

For the radio-based localization with WLAN, the radio map characterizes the RSS–position dependence through training

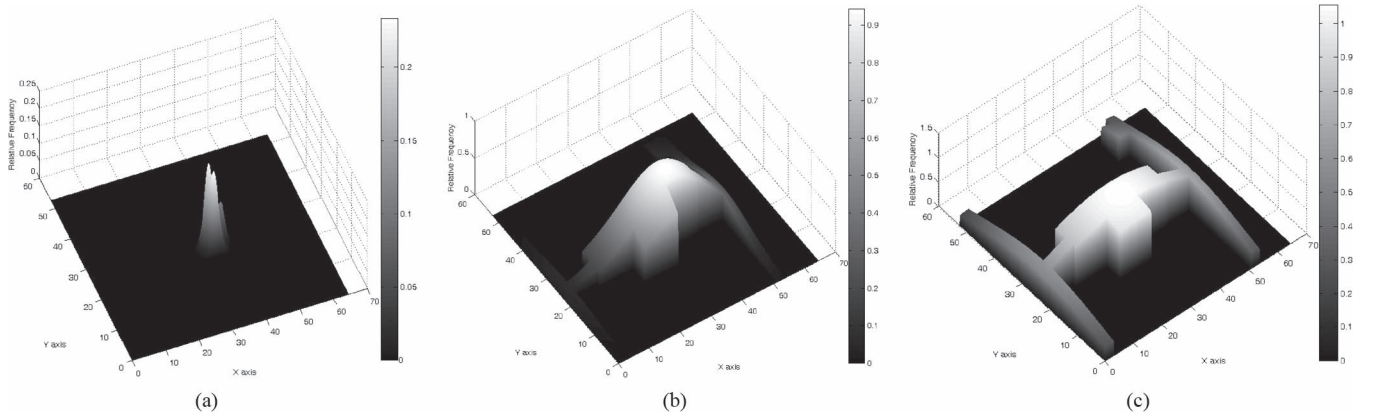

Fig. 4. Examples for KDE-based radio map models. Suppose we only select two APs for observation likelihood updating, if a particle is sampled at a point on the map with the corresponding measurement, the probability density is estimated by the kernel estimator with the local RSS information. Note that the vertical axis provides the likelihood probability with the Gaussian kernel. (a) Smooth factor $\sigma = 1$. (b) Smooth factor $\sigma = \sqrt{10}$. (c) Smooth factor $\sigma = \sqrt{20}$.

measurements at ANs [12], [26], [27], [30], [32], [33], [37]. The radio map model can be categorized into deterministic model and probabilistic model—the former associates with each AN point of the environment a mean RSS value for each node, and the latter represents a probability distribution of RSS values. The positioning techniques based on the deterministic radio map can be referred to as the location fingerprinting [16]. In contrast, the stochastic radio map is more realistic as it takes into account possible dynamic variations in the environment. To compare the localization performance, we not only propose a probabilistic approach using KDE but also address a deterministic method that applies the neural fuzzy system to the map interpolation.

A. Proposed Probabilistic Approach: KDE for Radio Map Modeling

In this paper, we propose a radio model based on an empirical RSS distribution using a KDE [40] due to its success in the approximation of probability density distributions. In addition, the radio model can be formed as a density function instead of an explicit measurement model to characterize the RSS–position relationship. Because the RSS distribution is spatially dependent, KDE can be used to infer the measurement contribution to the update according to the locally relevant training data information, which provides successful flexible density estimation with NLOS propagation. After choosing a subset of detectable APs using the SSMV algorithm, the index set $\mathcal{B}_{\text{index}}^{\min}$ of detectable APs presents the measurement $\mathbf{z}_k = \left[r_{k,B_1^{\min}}, \ldots, r_{k,B_m^{\min}}\right]^T$ for updating ALSPF from WLAN-RSS observations $\mathbf{r}_k$. The kernel density estimator requires a set of training pairs from radio map $\mathcal{R} = \{\mathbf{x}_{\text{tr}}^i, \mathbf{r}_\mu^i, \mathbf{r}_\sigma^i\}_{i=1}^{N_{\text{AN}}}$, which is used to comprise the training pairs selected by $\mathcal{B}_{\text{index}}^{\min}$. In order to approximate the observation likelihood model $p(\mathbf{z}_k|\mathbf{x}_k)$, a multivariate Gaussian kernel-based density estimation is used to evaluate the significance weight and is given as follows:

$$\omega_k^i = \frac{1}{N_{\text{AN}}} \sum_{i=1}^{N_{\text{AN}}} \frac{1}{\left(2\pi\sigma^2\right)^{1/2}} \exp\left(\frac{\left\|\boldsymbol{\xi}_k - \tilde{\boldsymbol{\xi}}_{\text{tr}}^i\right\|^2}{2\sigma^2}\right) \tag{20}$$

where

$$\boldsymbol{\xi}_k = \begin{bmatrix} x_k^i & y_k^i & (\mathbf{z}_k)^T \end{bmatrix}^T = \begin{bmatrix} x_k^i & y_k^i & r_{k,B_1^{\min}}, \ldots, r_{k,B_m^{\min}} \end{bmatrix}^T$$

is composed of the ith particle state and the online RSS observation $\mathbf{z}_k = \left[r_{k,B_1^{\min}}, \ldots, r_{k,B_m^{\min}}\right]^T$, which is produced by the SSMV algorithm, and $\sigma > 0$ is a smoothing parameter. In the preceding formulation, $p(\mathbf{z}_k|\mathbf{x}_k)$ is determined using a Gaussian mixture obtained from a spatially distributed set of sets, and the measurement equation is essentially replaced by the approximation. Fig. 4 demonstrates three examples of radio map modeling using KDE with different smoothing factors. It can be seen that the results from distributions of radio maps are adapted to the distinct RSS variation and NLOS problem [30] to provide the model robustness.

B. Deterministic Approach: Neural-Fuzzy-Based Radio Map Interpolation

The neural-fuzzy-based system ANFIS [34] allows a deterministic approach to interpolation problems, which is applied to interpolate the training data pairs of WLAN-RSS to achieve fine-grained radio map models. In the training phase, on the basis of radio map $\mathcal{R} = \{\mathbf{x}_{\text{tr}}^i, \mathbf{r}_\mu^i, \mathbf{r}_\sigma^i\}_{i=1}^{N_{\text{AN}}}$, the adaptive neuro fuzzy inference system (ANFIS)-based learning associates the inputs (AN positions x_{tr}^i) with the corresponding target (RSS mean value $\mathbf{r}_\mu^i$) to generate an interpolated RSS map. In the online phase, if given the input values x_1^* and x_2^*, a predicted RSS y^* is inferred via (21) through the trained ANFIS network's weights α and membership functions f [34], i.e.,

$$y^* = \frac{\alpha_1 \cdot f_1\left(x_1^*, x_2^*\right) + \alpha_2 \cdot f_2\left(x_1^*, x_2^*\right)}{\alpha_1 + \alpha_2}. \tag{21}$$

Then the observation likelihood $p(\mathbf{z}_k|\mathbf{x}_k)$ based on ANFIS is given as follows:

$$\omega_k^i = \frac{1}{\sqrt{2\pi}\sigma'} \exp\left(-\frac{\left\|\mathbf{z}_k - \bar{\mathbf{y}}\left(\mathbf{x}_k^i\right)\right\|^2}{2\sigma'^2}\right) \tag{22}$$

where σ' is a smooth factor, and $\overline{y}(x_k^i)$ is the expected RSS value found using (21) with the particle state vector $\mathbf{x}_k^i$, and $\mathbf{z}_k$ is the RSS measurement.

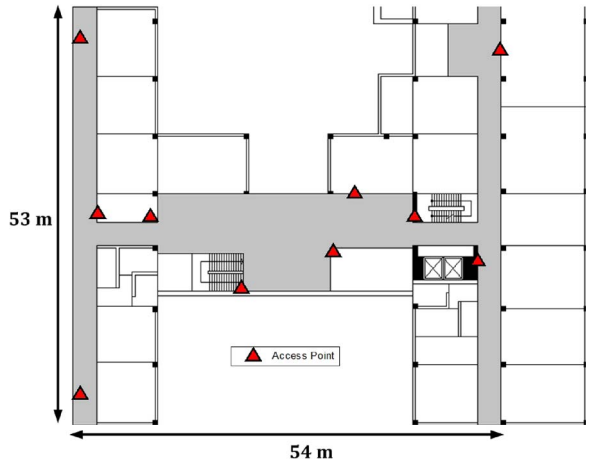

Fig. 5. Map of the experimentation site (53 m × 54 m). The gray region comprising the main hall and hallways is the area of interested and feasible area for robot traveling. The red triangles indicate the areas equipped with off-the-shelf APs; their locations are assumed to be unknown.

Both (20) and (22) are used for measurement update in the importance sampling stage to compute the particle weights. In addition, a feasible region $\mathcal{C}$ is adopted to filter the particles and renew the particle weight as follows:

$$\omega_k^i = \begin{cases} \omega_k^i, & \text{if } x_k^i \in \mathcal{C} \\ 0, & \text{otherwise.} \end{cases} \tag{23}$$

The proposed probabilistic approach utilizes the training data and KDE to calculate the probability and provide a continuous fine-grained radio map. Moreover, the KDE model was also simple enough for online computation without storing a large memory for map information and increasing the number of training pairs. On the contrary, the interpolation-based approach required long-term training effort for the interpolation procedure, in addition to a large number of training pairs and large memory storage to achieve a fine-grained map. The performance of the interpolation-based approach is limited as it is trained using only the specific deterministic target, i.e., the RSS mean value, which might induce the inappropriate RSS prediction results in NLOS propagation environments.

VI. Experiments and Results

This section describes the results of experiments conducted using the proposed robot localization method. The problem considered in the framework of this paper concerns low-density WLAN environment. Experiments were carried out on the first floor of the engineering building of National Chiao Tung University (Taiwan), as shown in Fig. 5. The dimensions of the experimentation region used for localization were 54 m × 53 m (2862 m^2), which is a bigger area than those used in [16], [20]–[22], [25], [28]–[31], and [33]. At the site of the experiment, commercial off-the-shelf APs whose coordinates were not needed were installed, and a smartphone was attached to the mobile robot to receive WLAN-RSS values for an acquisition program. In addition, we implemented all the algorithms in an industrial computer (2-GHz Intel Core2 central processing unit).

Fig. 6. Developed mobile robot in this paper.

Fig. 6 shows the wheelchair robot that was designed to provide user transportation service in WLAN environments. The sensors equipped on the robot are IMU, encoders, laser range finder, and ultrasonic sensors. Since the sampling times of the deployed sensors measuring RSS, velocity, and orientation are 2, 5, and 25 Hz, respectively, we set the system updating rate as 2 Hz. Our WiFi scanning can be implemented by software without additional hardware and will not increase the cost.

A. Training Data Set

We installed ten commercial off-the-shelf APs in the testbed, and each AN was covered by six APs on average, and at least two APs were detectable for some outlying areas on the map. In the testbed, WLAN-RSS values were collected for 236 ANs (training locations) with a separation of 2 m. For each AN, a total of 200 samples was collected at a sampling rate of 2 samples/s. The AN coordinates and measured offline RSS data were used to build the radio map $\mathcal{R} = \{\mathbf{x}_{\text{tr}}^i, \mathbf{r}_\mu^i, \mathbf{r}_\sigma^i\}_{i=1}^{N_{\text{AN}}}$, which is also called the RSS fingerprints. Please note that ANs for radio modeling should cover all the areas traversed by the robot. If the robot traverses a zone that has no radio map information, the estimator will be diverged from the current estimation due to the seriously mismatched RSS measurements.

B. Testing Data and Route Types

Test data were collected over three days and were separated from training days to reflect the mismatch between training and testing conditions in the real-life operation of the system and capture variations of environmental uncertainties. The test samples were collected for four types of test routes, which are summarized in Table IV and considered as follows.

1) *Simple transportation*: These routes consisted of straight paths from a source to a destination with turns at most 90° along the way.

2) *Pathway round trip*: This test case considered movement scenarios of the pathway with direction reversal such as moving from one office to another office and then back to the original office.
3) *Lobby round trip*: This case considered motion scenarios with a round trip for guidance service in a museum or at an art show.
4) *Entire floor round trip*: This test case considered scenarios that are a combination of the previous three scenarios, and the distance traveled was the longest one. R4 was examined for a wide variety of challenges in WLAN localization. This included the most limited partial coverage of sensors, the RSS interference, and the NLOS problem due to pedestrian bodies or unknown obstacles in the environment.

Consequently, the training sets were collected over the five days, and the test data were collected in the span of another three days. This setup ensured that the 11 800 training samples and 4600 testing samples were disjoint enough to provide realistic results. In addition, the average speed of the robot is 0.56 m/s. Therefore, the provided experimental scenarios and data sets were extensively comparable with related work [7], [8], [13], [15], [16], [21]–[23], [28], [29], [33].

C. Performance Metric

We adopted the distance error as the performance metric, which was evaluated using root-mean-square error (RMSE) with the Euclidean distance between the true position and its estimate. Therefore, the RMSE for the jth route, i.e., e_j, and the average RMSE (ARMSE), i.e., e_{avg}, are defined as follows:

$$e_j = \sqrt{\frac{1}{K_j}\sum_{k=1}^{K_j}(\hat{\mathbf{x}}_{k,j} - \mathbf{x}_k)^2} \tag{24}$$

$$e_{\text{avg}} = \frac{1}{N_R}\sum_{j=1}^{N_R} e_j \tag{25}$$

where x_k is the ground truth obtained by recording the traversed labels on the floor with a laser pointer equipped on the robot, $\hat{\mathbf{x}}_{k,j}$ is the estimate of $\mathbf{x}_k$ in the jth route, K_j is the length of the route, and N_R is the total number of the routes.

D. Localization Results and Performance Evaluation

In order to show the feasibility and suitability of the methods with a low sensor density, the experimental routes in Table III are examined. The radio signal quality is influenced by the mobile terminal movement; thus, the limitation of robot velocity should be clarified for the robustness and performance of radio robot localization. The robot speed in experiments is dynamically changed due to several motion behaviors in tasks, such as high-speed traveling in free space or slowly moving in crowded space and stop or turning. As can be observed in Table IV, the proposed algorithms are examined more strictly with a lower density WLAN environment. Moreover, the amount and the scenarios of the examined routes are complex and practical enough to be compared with related work on radio-based robot localization [10], [15], [16], [18], [21], [24].

TABLE III
TESTING ROUTES AND MOTION SCENARIO

Route scenario	Route index	Avg. length	Avg. velocity	Avg. detectable AP number
Simple transportation	R1	60.58m	0.54 m/s	6.69
Pathway round-trip	R2	80.00m	0.77 m/s	5.4
Lobby round-trip	R3	76.94 m	0.38 m/s	7.45
Entire floor round-trip	R4	276.70 m	0.57 m/s	5.82

In our work, we adopted $N_S = 500$ for ALSPF and set the time average window $T_{\text{ALS}} = 10$ for the ALS algorithm, and the threshold N_T (see Table I) is set to be 50 (10% of N_S). The implemented localization procedures were completed within 0.5 s, which provides real-time operation since the WLAN-RSS sampling rate was 2 Hz in this study.

1) Tracking Results: In Fig. 7, a visualized example (R4) is compared between the true trace and the estimated ones obtained by the proposed radio localization system. In the online estimation phase, while the mobile robot moves along the routes, the attached smartphone of robot measures the WLAN-RSS values from APs. After gathering the RSS observations, ALSPF updates the estimated coordinates of the mobile robot based on the KDE radio model with 2 APs selected by the SSMV algorithm. Fig. 7 presents a combination of all the motion scenarios by performing entire floor round trip; its starting point is located at point Ⓐ in the lobby. It can be seen that the proposed radio localization can track the mobile robot precisely in the WLAN environment; after such a long-term tracking, it was observed that good tracking was presented without accumulative errors.

Table V shows the error statistics of the tracking results achieved by ALSPF with the KDE model and SSMV AP selection for each motion test cases. The proposed approach effectively and successfully performs under varied movements, higher speed, and realistic noisy measurements induced by the limited partial coverage of APs, NLOS conditions due to walls, and multiple pedestrians. As a result, these cases reveal that the developed localization system is accurate and reliable in tracking the mobile robot under different motion scenarios.

2) Effect of AP Selection: Fig. 8 compares the ARMSE obtained from the ALSPF with respect to three AP selection schemes, namely, SSMV, strongest observation RSS [39], which is the most conventional approach, and random selection. The strongest criterion ranks APs in descending order of their RSS mean values, and the random criterion randomly selects a few of detectable APs regardless of their RSS values. In this context, the AP selection approaches that satisfy sufficient coverage of APs are inapplicable and not implemented in this study since there are only few detectable APs along the examined routes. Hence, different to related studies [25], [30], [31], [33], [39], this paper concerning a low AP density, the comparison of AP selection is based on 2–5 APs.

In this paper, the selection of SSMV algorithm is performed to choose the APs with respect to the minimum variance over

TABLE IV
COMPARISON OF EXAMINED EXPERIMENTS FOR RADIO-BASED ROBOT LOCALIZATION

Robot System	Testbed size (m^2)	Radio source	Radio sensor precise	Sensor density	Robot velocity (m/s)	Examined routes
This study	**2862**	**WLAN**	**Low**	**286.2 m^2/BS**	**0.56 (Average)**	**40**
Park [15]	26.4	RFID	High	0.13 m^2/tag	0.12 (Average)	3
Cho [21]	81	CSS	High	20.5 m^2/BS	0.3 (Average)	1
Cheng [22]	63	WSN and Ultrasonic	High	9.0 m^2/BS	Static	1
Song [24]	1.34	Ultrasonic sensor	High	0.335 m^2/BS	0.4 (Average)	3

Note: BS is the base station.

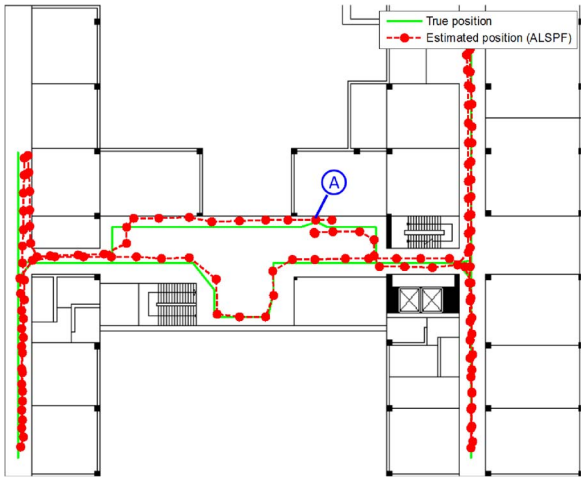

Fig. 7. Estimated trajectories of R4 using the proposed (dashed line) WLAN localization and (solid line) ground truth. The node Ⓐ is the starting location and the destination.

TABLE V
LOCALIZATION RESULTS FOR EACH TEST CASE

Test case	Total routes	Error mean (m)	Error std (m)	ARMSE (m)
Simple transportation	16	1.24	0.54	1.42
Pathway round-trip	16	1.26	0.66	1.52
Lobby round-trip	4	0.96	0.50	1.13
Entire floor round	4	0.86	0.73	1.35

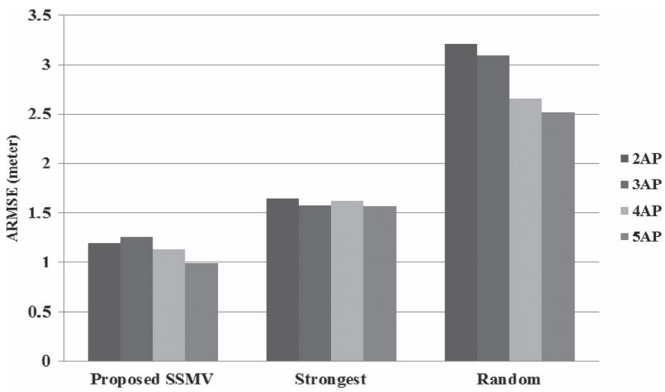

Fig. 8. Effect of adopted AP selection. The results are obtained by ALSPF with the KDE-based radio model.

the set of APs with the strongest RSS mean. Fig. 8 indicates that SSMV significantly outperforms the results of strongest and random selection in each case of deployed numbers. The performance degradation of the method with the strongest RSS is attributed to the redundant noise from the unstable APs.

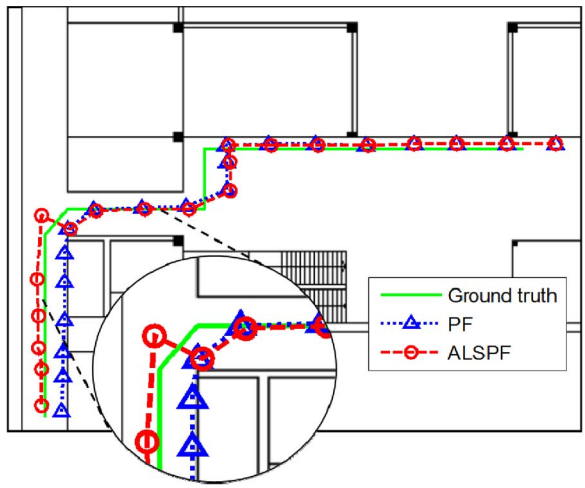

Fig. 9. Scatterplot of estimated locations (R1) with and without ALS algorithm.

Thus, we squeeze the useful information into the relatively lower dimension by a suitable AP rank provided by using SSMV. Only the selected APs are retained for robot localization. In addition, Fig. 8 shows that the proposed criterion outperforms other methods and utilizes the fewest APs set to achieve improvements of 0.45 m (27.43%), 0.33 m (21.02%), 0.49 m (30.24%), and 0.57 m (36.54%) over 2–5 APs, which, in turn, reduces the computational cost required by each location estimation. These indicate that SSMV effectively mitigates the imprecise APs and redundant noise.

3) Effect of ALS Algorithm: Fig. 9 compares the tracking results between PF and ALSPF based on the KDE model. In Fig. 9, after the mobile robot passed through the corner of the pathway, the estimated trajectory using PF is too close to the wall because failed prediction around the corner happens due to the fixed statistics of motion uncertainties, the major part of particles are degenerated and prematurely concentrated at a wrong point. Thus, the PF meets the IE while predicting an erroneous estimation at corner, and then, the PD occurs. Obviously, the trajectories of the PF deviate from ground truth; however, the ALS algorithm demonstrates better accuracy and robust performance because the IEs are removed, and it can successfully provide corrected estimates and motion uncertainties with the ALS algorithm instead of the global resampling. As a result, Fig. 9 presents the effectiveness of the ALS algorithm for the adaptive updating.

4) Effect of WLAN Density: Fig. 10 shows the effect of decreasing the number of detectable APs on positioning accuracy. The sensor density is a challenge of the robustness and accuracy for the radio-based localization. The low-sensor-density

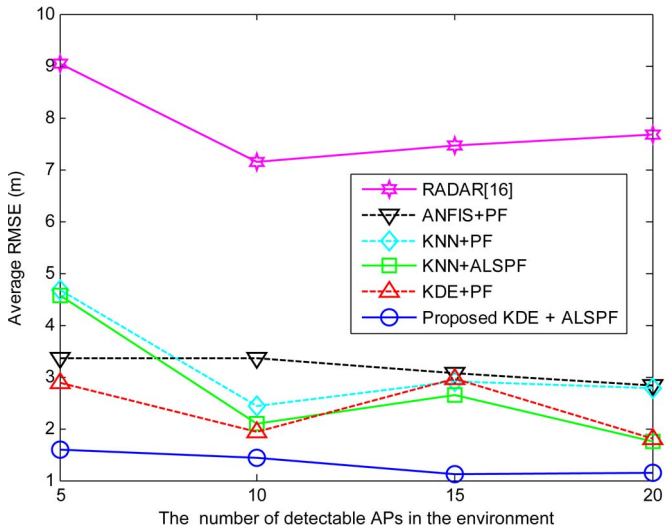

Fig. 10. ARMSE versus the number of APs in the experimental environment.

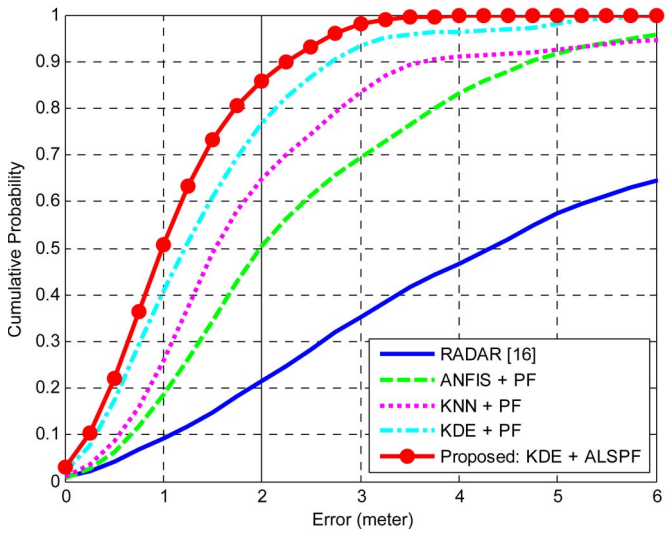

Fig. 11. Empirical cumulative probability of position errors.

conditions will degrade the performance in real operation of a positioning system. Please note that our positioning system only selects two APs from the detected AP set dynamically using the SSMV algorithm. For the lowest density, the proposed framework based on ALSPF with the KDE model achieved the high level of accuracy and demonstrates the best performance improvements of 1.28 m (44.46%), 3.07 m (64.96%), and 1.42 m (47%) over PF estimator with the KDE model, PF estimator with the ANFIS model, and PF estimator with the k-nearest neighbor (KNN) model. Therefore, these verified the robustness of the proposed approach.

E. Comparison With Other Methods

To quantify the effectiveness, the proposed localization system is compared with PF-based schemes with respect to different radio map models. To ensure fair comparison of algorithm performances, all methods use 500 particles and two APs selected by the SSMV-based AP selection. Fig. 11 and Table VI indicate that the ALSPF algorithm significantly outperforms the other methods. In particular, Table VI illustrates

TABLE VI
COMPARISON OF ARMSE RESULTS

Estimation Method	Radio Map Model	Error mean (m)	Error std (m)	ARMSE (m)
RADAR [16]	Training Pairs	6.04	5.03	7.84
PF	KNN [42]	2.18	0.89	2.44
	ANFIS [34]	2.50	1.39	2.96
	KDE	1.51	0.65	1.67
Proposed ALSPF	KNN [42]	1.41	0.89	1.72
	ANFIS [34]	2.05	1.01	2.31
	KDE	1.08	0.61	1.35

the improvement brought by the ALS algorithm. The ALSPF estimator achieves the improvements (ARMSE) with respect to the KDE, ANFIS, and KNN models of 0.24 m (16.78%), 0.97 m (37.59%), 1.12 m (49.39%) over the PF estimator based on the KDE, ANFIS, and KNN models, respectively. Furthermore, we can observe 86.08% improvement in ARMSE while applying our method to RADAR [16].

VII. CONCLUSION

A radio-based robot localization with low-density WLAN APs has been proposed in this paper. A new methodology based on location fingerprints with KDE is used to deal with the noisy data and environmental uncertainties and overcome the lack of an explicit measurement model. Moreover, two online strategies, i.e., SSMV AP selection and ALSPF, are proposed to enhance positioning accuracy. The SSMV algorithm can facilitate more efficient utilization of APs and be applied to deal with low-density situations by selecting more precise APs relatively. The unreasonable estimates can be removed by cooperating with the ALS algorithm and particle filtering that adaptively correct the robot location states in the importance sampling stage. To demonstrate the feasibility of the proposed localization system, we sufficiently examined the proposed algorithms by extremely low AP density, high-speed robot movements, several complex motion, and long-term routes.

The experimental results indicate that the proposed framework is robust to the number of deployed APs and confirms the effectiveness of ALSPF in improving accuracy when compared with PFs and other radio models. Consequently, the proposed new radio localization algorithms for mobile robots are successfully performed and can accurately track the position with low-density WLAN APs.

REFERENCES

[1] D. Lee and W. Chung, "Discrete-status-based localization for indoor service robots," *IEEE Trans. Ind. Electron.*, vol. 53, no. 5, pp. 1737–1746, Oct. 2006.
[2] W. Chung, C. Rhee, Y. Shim, H. Lee, and S. Park, "Door-opening control of a service robot using the multifingered robot hand," *IEEE Trans. Ind. Electron.*, vol. 56, no. 10, pp. 3975–3984, Oct. 2009.
[3] N. Bellotto and H. Huosheng, "Multisensor-based human detection and tracking for mobile service robots," *IEEE Trans. Syst., Man, Cybern. B, Cybern.*, vol. 39, no. 1, pp. 167–181, Feb. 2009.
[4] K. H. Park, H. E. Lee, Y. Kim, and Z. Z. Bien, "A steward robot for human-friendly human–machine interaction in a smart house environment," *IEEE Trans. Autom. Sci. Eng.*, vol. 5, no. 1, pp. 21–25, Jan. 2008.
[5] A. T. de Almeida and J. Fong, "Domestic service robots," *IEEE Robot. Autom. Mag.*, vol. 18, no. 3, pp. 18–20, Sep. 2011.

[6] G. Song, K. Yin, Y. Zhou, and X. Cheng, "A surveillance robot with hopping capabilities for home security," *IEEE Trans. Consum. Electron.*, vol. 55, no. 4, pp. 2034–2039, Nov. 2009.
[7] A. Mihailidis, P. Elinas, J. Boger, and J. Hoey, "An intelligent powered wheelchair to enable mobility of cognitively impaired older adults: An anticollision system," *IEEE Trans. Neural Syst. Rehab. Eng.*, vol. 15, no. 1, pp. 136–143, Mar. 2007.
[8] K. C. Chen and W. H. Tsai, "Vision-based autonomous vehicle guidance for indoor security patrolling by a SIFT-based vehicle-localization technique," *IEEE Trans. Veh. Technol.*, vol. 59, no. 7, pp. 3261–3271, Sep. 2010.
[9] A. I. Mourikis, S. I. Roumeliotis, and J. W. Burdick, "SC-KF mobile robot localization: A stochastic cloning Kalman filter for processing relative-state measurements," *IEEE Trans. Robot.*, vol. 23, no. 4, pp. 717–730, Aug. 2007.
[10] E. DiGiampaolo and F. Martinelli, "Mobile robot localization using the phase of passive UHF RFID signals," *IEEE Trans. Ind. Electron.*, vol. 61, no. 1, pp. 365–376, Jan. 2014.
[11] F. Gustafsson and F. Gunnarsson, "Mobile positioning using wireless networks: Possibilities and fundamental limitations based on available wireless network measurements," *IEEE Signal Process. Mag.*, vol. 22, no. 4, pp. 41–53, Jul. 2005.
[12] H. Liu, H. Darabi, P. Banerjee, and J. Liu, "Survey of wireless indoor positioning techniques and systems," *IEEE Trans. Syst., Man, Cybern. C, Appl. Rev.*, vol. 37, no. 6, pp. 1067–1080, Nov. 2007.
[13] S. S. Saab and Z. S. Nakad, "A standalone RFID indoor positioning system using passive tags," *IEEE Trans. Ind. Electron.*, vol. 58, no. 5, pp. 1961–1970, May 2011.
[14] M. S. Arulampalam, S. Maskell, N. Gordon, and T. Clapp, "A tutorial on particle filters for online nonlinear non-Gaussian Bayesian tracking," *IEEE Trans. Signal Process.*, vol. 50, no. 2, pp. 174–188, Feb. 2002.
[15] S. Park and S. Hashimoto, "Autonomous mobile robot navigation using passive RFID in indoor environment," *IEEE Trans. Ind. Electron.*, vol. 56, no. 7, pp. 2366–2373, Jul. 2009.
[16] P. Bahl and V. N. Padmanabhan, "Radar: An in-building RF-based user location and tracking system," in *Proc. IEEE INFOCOM*, 2000, vol. 2, pp. 775–784.
[17] B. S. Choi, J. W. Lee, J. J. Lee, and K. T. Park, "A hierarchical algorithm for indoor mobile robot localization using RFID sensor fusion," *IEEE Trans. Ind. Electron.*, vol. 58, no. 6, pp. 2226–2235, Jun. 2011.
[18] B. S. Choi and J. J. Lee, "Sensor network based localization algorithm using fusion sensor-agent for indoor service robot," *IEEE Trans. Consum. Electron.*, vol. 56, no. 3, pp. 1457–1465, Aug. 2010.
[19] S. S. Saab and Z. S. Nakad, "Inertial sensor-based indoor pedestrian localization with minimum 802.15.4a configuration," *IEEE Trans. Ind. Informat.*, vol. 7, no. 3, pp. 455–466, Aug. 2011.
[20] J. Wang, Q. Gao, Y. Yu, H. Wang, and M. Jin, "Toward robust indoor localization based on Bayesian filter using chirp-spread-spectrum ranging," *IEEE Trans. Ind. Electron.*, vol. 59, no. 3, pp. 1622–1629, Mar. 2012.
[21] H. Cho and S. W. Kim, "Mobile robot localization using biased chirp-spread-spectrum ranging," *IEEE Trans. Ind. Electron.*, vol. 57, no. 8, pp. 2826–2835, Aug. 2010.
[22] L. Cheng, C. D. Wu, and Y. Z. Zhang, "Indoor robot localization based on wireless sensor networks," *IEEE Trans. Consum. Electron.*, vol. 57, no. 3, pp. 1099–1104, Aug. 2011.
[23] S. J. Kim and B. K. Kim, "Accurate hybrid global self-localization algorithm for indoor mobile robots with two-dimensional isotropic ultrasonic receivers," *IEEE Trans. Instrum. Meas.*, vol. 60, no. 10, pp. 3391–3404, Oct. 2011.
[24] H. Song, V. Shin, and M. Jeon, "Mobile node localization using fusion prediction based interacting multiple model in cricket sensor network," *IEEE Trans. Ind. Electron.*, vol. 59, no. 11, pp. 4349–4359, Nov. 2012.
[25] S. H. Fang and T. Lin, "Principal component localization in indoor WLAN environments," *IEEE Trans. Mobile Comput.*, vol. 11, no. 1, pp. 100–110, Jan. 2012.
[26] S. H. Fang, T. N. Lin, and P.-C. Lin, "Location fingerprinting in a decorrelated space," *IEEE Trans. Knowl. Data Eng.*, vol. 20, no. 5, pp. 685–691, May 2008.
[27] S. H. Fang and C. H. Wang, "A dynamic hybrid projection approach for improved Wi-Fi location fingerprinting," *IEEE Trans. Veh. Technol.*, vol. 60, no. 3, pp. 1037–1044, Mar. 2011.
[28] A. M. Ladd, K. E. Bekris, A. P. Rudys, D. S. Wallach, and L. E. Kavraki, "On the feasibility of using wireless Ethernet for indoor localization," *IEEE Trans. Robot. Autom.*, vol. 20, no. 3, pp. 555–559, Jun. 2004.
[29] S. P. Kuo and Y. C. Tseng, "Discriminant minimization search for large-scale RF-based localization systems," *IEEE Trans. Mobile Comput.*, vol. 10, no. 2, pp. 291–304, Feb. 2011.
[30] A. Kushki, K. N. Plataniotis, and A. N. Venetsanopoulos, "Intelligent dynamic radio tracking in indoor wireless local area networks," *IEEE Trans. Mobile Comput.*, vol. 9, no. 3, pp. 405–419, Mar. 2010.
[31] Y. Chen, J. Yin, X. Chai, and Q. Yang, "Power-efficient access-point selection for indoor location estimation," *IEEE Trans. Knowl. Data Eng.*, vol. 18, no. 7, pp. 877–888, Jul. 2006.
[32] S. H. Fang and T. Lin, "Projection-based location system via multiple discriminant analysis in wireless local area networks," *IEEE Trans. Veh. Technol.*, vol. 58, no. 3, pp. 5009–5019, Nov. 2009.
[33] A. Cenedese, G. Ortolan, and M. Bertinato, "Low-density wireless sensor networks for localization and tracking in critical environments," *IEEE Trans. Veh. Technol.*, vol. 59, no. 6, pp. 2951–2962, Jul. 2010.
[34] J. S. Jang, "ANFIS: Adaptive-network-based fuzzy inference system," *IEEE Trans. Syst., Man, Cybern.*, vol. 23, no. 3, pp. 665–685, May/Jun. 1993.
[35] B. F. Wu, C. L. Jen, and K. C. Chang, "Neural fuzzy based indoor localization by Kalman filtering with propagation channel modeling," in *Proc. IEEE Int. Conf. Syst., Man, Cybern.*, Montreal, QC, Canada, Dec. 7–10, 2007, pp. 812–817.
[36] B. F. Wu, C. L. Jen, and T.-W. Huang, "The graphic feature node based dynamic path planning and fuzzy based navigation for intelligent wheelchair robots," *J. Convergence Inf. Technol.*, vol. 8, no. 11, pp. 194–203, 2013.
[37] B. F. Wu, C. L. Jen, and T. W. Huang, "Intelligent radio based positioning and fuzzy based navigation for robotic wheelchair with wireless local area networks," in *Proc. IEEE Int. Conf. Robot, Vis. Signal Process.*, Taiwan, Nov. 2011, pp. 61–64.
[38] J. Biswas and M. Veloso, "WiFi localization and navigation for autonomous indoor mobile robots," in *Proc. IEEE Int. Conf. Robot. Autom.*, May 3–8, 2010, pp. 4379–4384.
[39] M. Youssef, A. Agrawala, and A. U. Shankar, "WLAN location determination via clustering and probability distributions," in *Proc. IEEE Pervasive Comput. Commun.*, 2003, pp. 143–150.
[40] B. Silverman, *Density Estimation for Statistics and Data Analysis*. London, U.K.: Chapman & Hall, 1986.
[41] D. W. Scott, *Multivariate Density Estimation*. Hoboken, NJ, USA: Wiley, 1992.
[42] T. Hastie, R. Tibshirani, and J. Friedman, *The Elements of Statistical Learning: Data Mining, Inference, Predictions*, 2nd ed. New York, NY, USA: Springer-Verlag, 2009.

Bing-Fei Wu (S'89–M'92–SM'02–F'12) received the B.S. and M.S. degrees in control engineering from National Chiao Tung University (NCTU), Hsinchu, Taiwan, in 1981 and 1983, respectively, and the Ph.D. degree in electrical engineering from the University of Southern California, Los Angeles, CA, USA, in 1992.

Since 1992, he has been with the Department of Electrical Engineering, NCTU, where he became a Professor in 1998 and a Distinguished Professor in 2010 and has been the Director of the Institute of Electrical Control Engineering since 2011. His research interests include image recognition, vehicle driving safety and control, intelligent robotic systems, and intelligent transportation systems.

Dr. Wu founded and served as the Chair of the Taipei Chapter of the IEEE Systems, Man, and Cybernetics Society (SMCS) in 2003. He has been the Chair of the Technical Committee on Intelligent Transportation Systems of the IEEE SMCS since 2012. He serves as an Associate Editor of the IEEE TRANSACTIONS ON SYSTEMS, MAN, AND CYBERNETICS: SYSTEMS.

Cheng-Lung Jen received the B.S. degree in electrical engineering from National Chin-Yi University of Technology, Taichung, Taiwan, in 2004, the M.S. degree in electrical engineering from National Central University, Jhongli, Taiwan, in 2006, and the Ph.D. degree in electrical control engineering from National Chiao Tung University, Hsinchu, Taiwan, in 2013.

He is currently with the Institute of Electrical Control Engineering, National Chiao Tung University. His main research interests are in the areas of machine learning, computer vision, wireless positioning systems, and mobile robotics.